VALIDATION OF NASCAP-2K SPACECRAFT-ENVIRONMENT INTERACTIONS CALCULATIONS

V.A. Davis
Science Applications International Corporation
10260 Campus Point Dr., M.S. A1
San Diego, CA, 92121
Phone: 858-826-1608
Fax: 858-826-1652
E-mail: victoria.a.davis@saic.com

M.J. Mandell
B.M. Gardner
I.G. Mikellides
Science Applications International Corporation

L.F. Neergaard
Jacobs Sverdrup Technology

D.L. Cooke
Air Force Research Laboratory/VSBS

J. Minor
NASA Marshall Space Flight Center

Abstract

The recently released *Nascap-2k*, version 2.0, three-dimensional computer code models interactions between spacecraft surfaces and low-earth-orbit, geosynchronous, auroral, and interplanetary plasma environments. It replaces the earlier three-dimensional spacecraft interactions codes NASCAP/GEO, NASCAP/LEO, POLAR, and DynaPAC. *Nascap-2k* has improved numeric techniques, a modern user interface, and a simple, interactive satellite surface definition module (Object ToolKit).

We establish the accuracy of *Nascap-2k* both by comparing computed currents and potentials with analytic results and by comparing *Nascap-2k* results with published calculations using the earlier codes. *Nascap-2k* predicts Langmuir-Blodgett or Parker-Murphy current collection for a nearly spherical (100 surfaces) satellite in a short Debye length plasma depending on the absence or presence of a magnetic field. A low fidelity (in geometry and time) *Nascap-2k* geosynchronous charging calculation gives the same results as the corresponding low fidelity NASCAP/GEO calculation. A high fidelity calculation (using the *Nascap-2k* improved geometry and time stepping capabilities) gives higher potentials, which are more consistent with typical observations. *Nascap-2k* predicts the same current as a function of applied potential as was observed and calculated by NASCAP/LEO for the SPEAR I rocket with a bipolar sheath. A *Nascap-2k* DMSP charging calculation gives results similar to those obtained using POLAR and consistent with observation.

Introduction

The three-dimensional spacecraft plasma environment interactions computer code *Nascap-2k*[1, 2, 3, 4] version 2.0 has recently been released. *Nascap-2k* computes a wide variety of plasma phenomena. These include spacecraft charging in geosynchronous, interplanetary, auroral, and low-earth-orbit plasmas, volume potentials, particle trajectories, and resulting variations in plasma density. The user interface is designed so that the non-expert user can do common problems and the expert can tackle questions that have not been previously contemplated. *Nascap-2k* takes advantage of improvements in computer technology, advances in understanding of the phenomena, and enhanced charging algorithms to improve upon the earlier three-dimensional computer codes. (NASCAP/GEO,[5, 6, 7, 8] NASCAP/LEO,[9, 10, 11, 12, 13] POLAR,[14] and DynaPAC[15, 16, 17]). While each code works well for the range of problems for which it was designed, by today's standards, these codes are complicated to use and require expertise to use properly. In addition NASCAP/GEO and POLAR are limited with respect to geometry. *Nascap-2k* builds on our experience with these codes and is designed to address their limitations. It incorporates all of the DynaPAC computational modules.

Previous papers have described *Nascap-2k*,[1, 2, 3, 4] its algorithms, and the new numeric techniques used. This paper focuses on comparison of *Nascap-2k* results with analytic solutions and with the results of NASCAP/GEO, NASCAP/LEO, and POLAR calculations.

Current Collection by a Sphere

We first validate that *Nascap-2k* reproduces analytic results for current collection by a sphere in a dense plasma. *Nascap-2k* incorporates the algorithms developed for NASCAP/LEO to model charge density and current collection in plasmas with Debye lengths short with respect to the mesh size of the calculational grid.[11, 14, 18, 19]

Nascap-2k provides a number of charge density models to use when solving Poisson's equation to obtain volume potentials. These include both analytic functions of the potential (and local electric field) and various combinations of tracked particle densities and analytic functions (such as the sum of a tracked ion density and a barometric function for electrons). In a dense plasma, when the spacecraft velocity and Earth's magnetic field have minimal effect on the charge density within the sheath, the non-linear analytic formula developed for NASCAP/LEO[11, 18] is generally appropriate. This analytic function of the potential smoothly interpolates between linear Debye screening at low potentials and the charge density of a single accelerated and converging species at high potentials.

$$\rho/\varepsilon_0 = -\left(\phi/\lambda_{nl}^2\right)\frac{\max\left(1, C\left(\phi, E\right)\right)}{1+\sqrt{4\pi}\left|\phi/\theta_{nl}\right|^{3/2}} \qquad \left(R_{sh}/r\right)^2 = 2.29\left|E\lambda_{nl}/\theta_{nl}\right|^{1.262}\left|\theta_{nl}/\phi\right|^{0.509}$$

$$C\left(\phi, E\right) = \min\left(\left(R_{sh}/r\right)^2, 3.545\left|\phi/\theta_{nl}\right|^{3/2}\right) \qquad \lambda_{nl^2} = \max(\lambda_{Debye}^2/g, D^2)$$

$$\theta_{nl} = \theta(\lambda_{nl}^2 g/\lambda_{Debye}^2)^{2/3}$$

where the symbols refer to the local potential, ϕ, the local electric field, E, the plasma temperature, θ, the debye length, λ_{debye}, the local mesh spacing, D, and the local reduction in plasma density due to wake effects (neutral model), g.

Generally the charge density is multiplied by a convergence factor, C, which is a function of the local potential and electric field. This factor accounts for the increase in charge density as charged particles from a large area are attracted to a small region. The function was developed to fit the results of Langmuir and Blodgett[20] for current collection by a sphere.

Current is computed by tracking macroparticles from a sheath edge. The sheath is the region from which the repelled species is excluded. Because the sheath absorbs the attracted species, the density of the attracted particles at the sheath edge is one-half the ambient plasma density. By quasi-neutrality, the density of the repelled species is the same, giving a sheath edge potential of $\phi_s = \pm\theta \ln\left(n/n_o\right) = \pm\theta \ln\left(0.5\right)$.

The charge stabilization algorithm,[14, 19] which makes solution of Poisson's equation possible in these dense plasmas, limits the potential drop in a single volume element. In the lowest potential regions of the computational space, this leads to computed potentials dropping off more slowly than the real potentials. This would lead to an error in the physical location of the sheath edge. To account for this, the calculation places the sheath edge at a potential that depends on the mesh size of the grid within which the sheath falls.

The current density through the sheath is the one-sided plasma thermal current, $J = e\,n\sqrt{\frac{e\phi}{2\pi m}}$.

Langmuir and Blodgett[20] analytically solved for the current collected by a biased sphere. Figure 1 shows the current collected by a sphere as a 0.1 m radius function of density as computed using Langmuir and Blodgett's results and by *Nascap-2k*. Figure 2 shows the current collected as a function of potential. *Nascap-2k* reproduces the Langmuir-Blodgett results.

In the presence of a significant magnetic field, the collected current is reduced. Parker and Murphy[21] developed an upper limit on the amount of current that can be collected in the limit of zero temperature and cylindrical symmetry. They accounted for the difficulty of attracting current into the sheath across magnetic field lines. *Nascap-2k* includes the magnetic field in

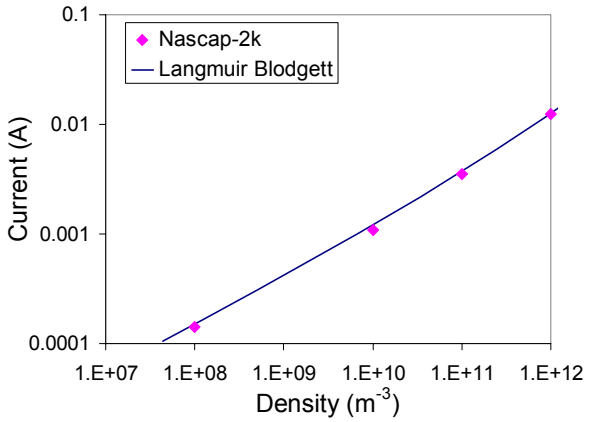

Figure 1. Electron current collected by a 100 V sphere from a 0.2 eV plasma, for no magnetic field.

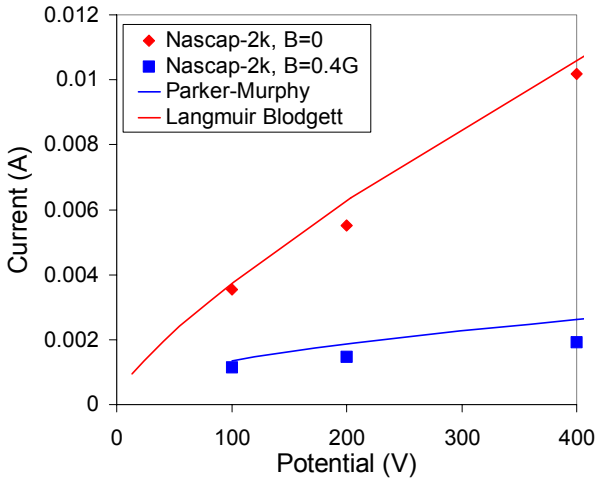

Figure 2. Electron current collected by a sphere from a 1011 m–3, 0.2 eV plasma.

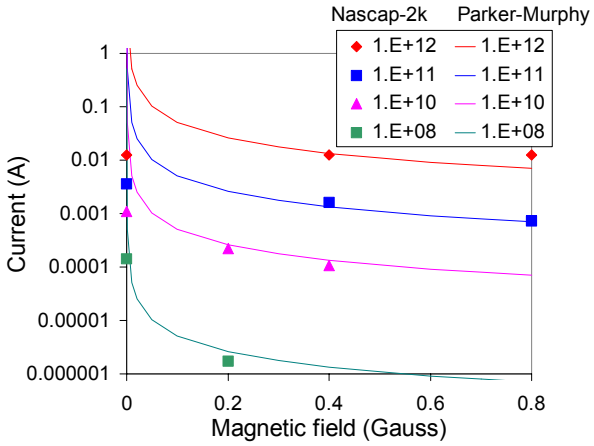

Figure 3. Electron current collected by a 100 V sphere from a 0.2 eV plasma. Densities are in m^{-3}.

Table 1. 90% worst case environment for geosynchronous orbits as defined in Reference 24.

	Temperature (keV)	Density (cm^{-3})
Ions	29.5	0.236
Electrons	12.0	1.12

current calculations in two ways. First, the magnetic field is included in the computation of macroparticle trajectories. With high magnetic fields, some of the particle trajectories that start at the sheath edge leave the sheath and cross the problem boundaries and other particles circle within the sheath and are never collected. Physically, these trapped particles provide an increased charge density that shrinks the sheath, thus reducing the current. However, this effect is *not* included in the analytic non-linear charge density model. The second way the magnetic field enters *Nascap-2k* calculations is when the Larmor radius exceeds the mesh size of the outer most grid by a factor of two, *Nascap-2k* reduces the sheath current by the cosine of the angle between the magnetic and electric fields. This accounts for the reduction of current to the sheath across magnetic field lines.

Figure 3 compares the current collected by a 0.1 m radius sphere as a function of magnetic field for a range of densities. Figure 2 shows the current collected as a function of sphere potential for a 0.4 Gauss magnetic field. The 10^{12} m^{-3} calculations were done with a small grid and *Nascap-2k* computed the sheath current in the same manner as in the absence of a magnetic field. In all the other calculations, the cross field sheath current was reduced. The *Nascap-2k* calculations are in agreement with the Parker-Murphy limits.

Charging in a Geosynchronous Plasma[22]

To validate *Nascap-2k* for geosynchronous charging calculations, we compare potentials computed using *Nascap-2k* with those computed with the industry standard NASCAP/GEO. To further illustrate the differences, we also compare the results with those obtained using the SEE Interactive Spacecraft Charging Handbook.[4, 23] The SEE Handbook is an interactive spacecraft charging code for the non-expert. It computes spacecraft surface charging for geosynchronous

and auroral zone spacecraft along with internal charging due to the deposition of high-energy (MeV) electrons.

A very simple spacecraft geometry, illustrated in Figure , was created to facilitate the comparison. The orientation of the solar arrays is appropriate to a spacecraft at 6 am local time. The proportions of the spacecraft were chosen to fit neatly in the NASCAP/GEO grid structure. The proportions of actual spacecraft almost always must be distorted in order to fit within the 17 x 17 x 33 grid. The SEE Handbook and *Nascap-2k* do not have this constraint.

The calculations use the environment recommended in Reference 24 (see Table 1) for initial modeling during the spacecraft design process. The spacecraft charges for 15 minutes, which is longer than any spacecraft would be exposed to such a severe environment.

The sun is taken to be incident on the spacecraft from the (0.92, 0.39, –0.02) direction. This is appropriate to a spacecraft in geosynchronous orbit at 0 longitude at 6 am GMT on January 1, 2000, consistent with the geometry model.

An important part of defining any spacecraft charging calculation is the determination of the appropriate values to use for the material properties for each surface. NASCAP/GEO, the SEE Handbook, and *Nascap-2k* all use the same fourteen material properties and incorporate them into the calculation in the same way. The focus here is in understanding variations between the results given by these codes. Therefore, the specific values are not important as long as they are consistent. We use the *Nascap-2k* provided default values for all the materials except the non-conducting paint on the antenna. For these surfaces, the values for Npaint[5] provided as a default material of NASCAP/GEO are used.

NASCAP/GEO calculations are done within a nested grid structure, with the innermost main grid 17 x 17 x 33 units in size. With the exception of booms that can extend beyond the

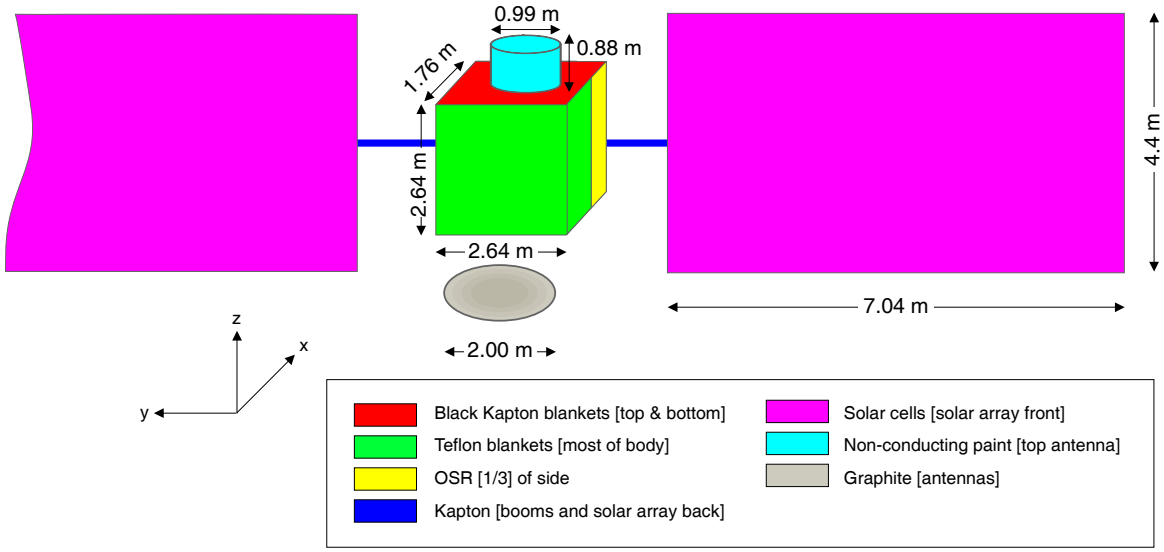

Figure 4. Illustrative spacecraft used for comparison of *Nascap-2k*, NASCAP/GEO, and SEE Interactive Spacecraft Charging Handbook.

main grid, the complete object must fit within this main grid. The object is made up of cubes, plates, wedges, tetrahedrons, and what is left of a cube after a tetrahedron is cut off of it. Booms (long cylindrical projections of arbitrary radius) can also be used. Booms must extend along the X, Y, or Z direction. Figure shows potentials on the best fidelity model that can be made. The Optical Solar Reflector (OSR) area is one-half rather than two-thirds of the spacecraft side and a cube represents the omni antenna. Actual spacecraft require even more distortion in order to fit them within the grid.

The SEE Handbook sets the location of each of the components. The user has no control over the distance between the various components or the zoning. This was done in order to insure stability and reasonable calculation speed in the tool, which is intended for general investigations. The orientation of the solar arrays is set by the longitude, date, and time.

Nascap-2k has a flexible geometric modeling capability. The user can control the size, shape, and gridding of each component. The omni antenna is represented by an octagonal cylinder and the side antennas are concave dishes.

The calculations were set up for 99 timesteps for a time period of 1000 seconds. The timesteps were chosen in the way most natural for each code. The NASCAP/GEO calculation uses geometrically growing timesteps starting with 1 second, with subsequent timesteps of 1.045 times the previous timestep. The SEE Handbook uses geometrically-distributed timesteps that the user cannot control. For the *Nascap-2k* calculation, we used the default geometrically distributed timesteps with a minimum of 0.1 seconds and a maximum of 60 seconds.

Table 2 compares the time required for an expert user to build a model and set up a calculation. This does *not* include the time needed to determine the most reasonable parameters for a specific problem. The determination of the appropriate material properties, geometry, environment, and calculation parameters for an actual analysis is typically days to weeks. It takes approximately as long to build a *Nascap-2k* model as to build a NASCAP/GEO model. However, the model created has the actual geometry and the resolution required. Sometimes it is necessary to build two NASCAP/GEO models at different resolutions in order to resolve questions.

The results of these sample calculations are summarized in Table 3. The potentials at 1000 seconds are shown in Figure 5 through Figure 7. The three codes give consistent results. The least negative surfaces are the ends of the solar arrays. The shaded Teflon surfaces are the most negative. All the surfaces that are more negative than the chassis are shaded insulators. In the center of the sun-facing side of the spacecraft body, the Teflon is slightly positive with respect to the chassis. This is most pronouced in the highest resolution *Nascap-2k* model. The sunlit insulators on the body are near the chassis potential or positive with respect to the chassis.

With the exception of the solar arrays, the surface potentials computed by the three codes are within approximately 35% of each other. The differences are primarily driven by the difference in the chassis potential. At the ends of the solar arrays, where the conductivity of the coverglass and barrier formation dominate the relative potentials, the differential potentials predicted by all three codes are within 4%. At the inner edges of the solar arrays, where the geometry is complex, the differentials vary by almost a factor of two between the minimum and the maximum.

There are two main contributions to differences between the solutions obtained using these three codes: resolution of the geometry and time fidelity.

In order to obtain a stable solution, the variation of the potential within a single timestep is limited. The algorithms for this limiting are complex and different for each of these codes. The SEE Handbook uses a strong limiting algorithm in order to ensure that the results are stable for a wide variety of problems. In NASCAP/GEO the limiting is partially under user control and moderate limiting (the default) was used for this calculation. *Nascap-2k* uses much less stabilization as the user is assumed to understand the code well enough to make the appropriate adjustments in the number and distribution of the timesteps in order to obtain a stable solution. As can be seen in Figure 8, the charging in *Nascap-2k* is faster than in either of the other two codes.

Table 2. Comparison of ease of use.

Code	Number of surfaces	Time to build model (min)	Time to set up calculation (min)	Time for charging calculation to complete on 800 MHz PC (min)
NASCAP/GEO	296	30	5	0.8
SEE Handbook	166	15	2	2
Nascap-2k	623	30	3	12

Table 3. Results of NASCAP/GEO, *Nascap-2k*, and SEE Handbook calculations, given in kV.

	Chassis	Kapton	OSR	Solar Cells	Teflon	Non-conducting paint
Absolute potentials (kV)						
NASCAP/GEO	–10.0	–8.2 to –13.1	–8.23 to –10.7	–5.2 to –7.68	–7.5 to –12.7	–8.3 to –10.3
SEE Handbook	–8.6	none in model	–7.3 to –9.6	–3.6 to –5.7	–6.8 to –11.3	–7.5 to –8.9
Nascap-2k	–12.0	–11.5 to –14.4	–10.0 to –13.7	–7.2 to –10.8	–7.9 to –14.0	–10.0 to –12.2
Differential potentials (kV)						
NASCAP/GEO		1.8 to –3.1	1.77 to –0.7	4.8 to 2.3	2.5 to –2.7	1.7 to –0.3
SEE Handbook		none in model	1.3 to –1.0	5 to 2.9	1.8 to –2.7	1.1 to –0.3
Nascap-2k		0.5 to –2.4	2 to –1.7	4.8 to 1.2	4.1 to –2	2 to –0.2

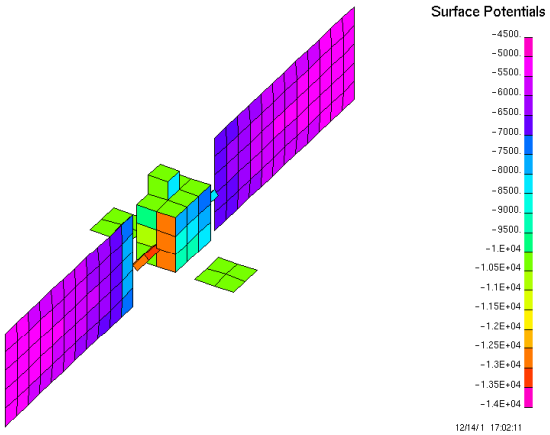

Figure 5. Results of spacecraft charging calculation using NASCAP/GEO.

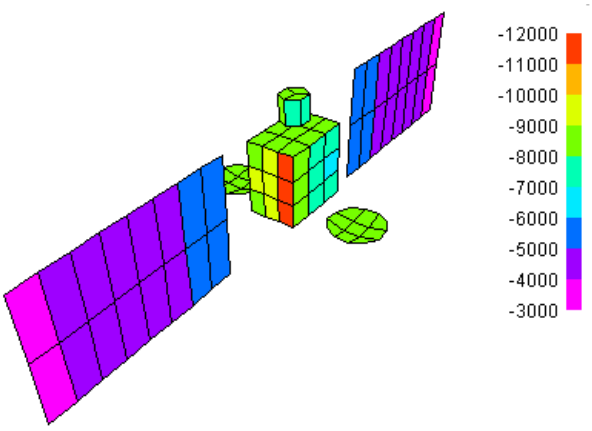

Figure 6. Results of spacecraft charging calculation using SEE Handbook.

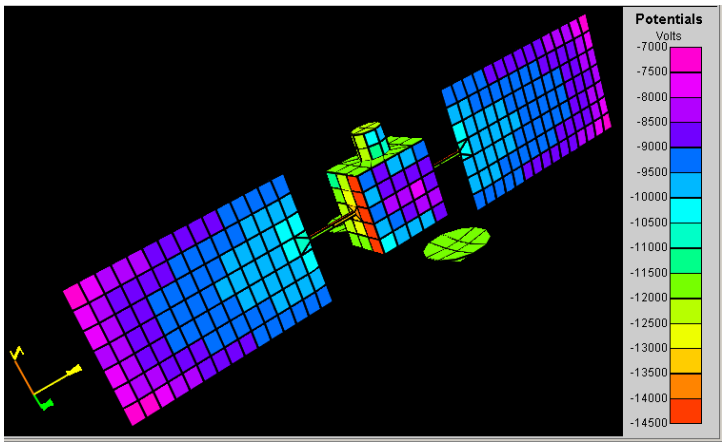

Figure 7. Results of spacecraft charging calculation using Nascap-2k.

The importance of geometric resolution can be illustrated by a comparison of the equilibrum solution given by the three codes as shown in Table 4. In order to further understand the differences due to geometry, a *Nascap-2k* object very similar to the SEE Handbook object was built and *Nascap-2k* used to compute potentials on it. The maximum negative differential in the NASCAP/GEO and *Nascap-2k* calculations are on the Kapton booms supporting the solar arrays. The SEE Handbook model and the simplified *Nascap-2k* model do not have these booms and the maximum negative differential potential is smaller than in the other cases. The chassis potentials computed by all three codes are within 13% of each other. The maximum positive differential potential is on the ends of the solar arrays. After 15 minutes of charging, all three codes give 5 kV differential. At equilibrum, the results are within 30% of each other. Most of this difference appears to be due to the differences in the geometric resolution, as the *Nascap-2k* calculation with the simplified model gives a differential closer to the SEE Handbook than the full geometry model. In all cases the maximum positive differential is about half of the chassis potential.

Nascap-2k improves our ability to model spacecraft surface charging, including improved geometric resolution and time fidelity. The surface charging calculated by *Nascap-2k* using low geometric and time fidelity is similar to the charging calculated by NASCAP/GEO.

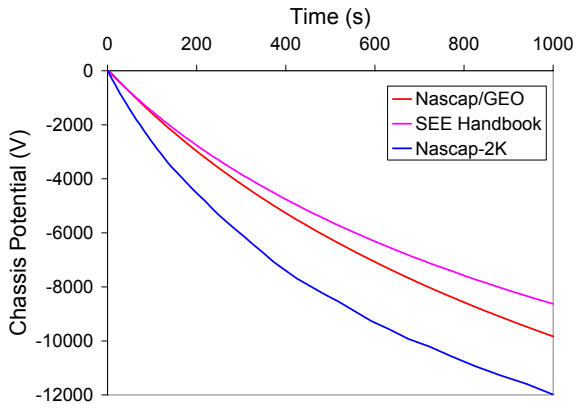

Figure 8. Comparison of chassis potential versus charging time as computed by NASCAP/GEO, SEE Handbook, and *Nascap-2k*.

Table 4. Comparison of equilibrum solutions (kV).

	Chassis	Max Differential	
		Positive	Negative
NASCAP/GEO	–20.3	10.8	–2.5
SEE Handbook	–17.8	10.4	–0.14
Nascap-2k	–19.5	7.8	–3.6
***Nascap-2k* with Handbook object**	–19.2	9.4	–0.06

Potentials and Currents in Dense Plasmas

A common issue on low-earth-orbit spacecraft is the prediction and control of interactions between a spacecraft with high-voltage components (ranging from a few volts to kilovolts) and the ionospheric environment. Since electron guns were first placed on rockets, the voltage on the main body necessary to collect ionospheric electrons and complete the circuit has been the subject of numerous theoretical and experimental studies. A large-scale effort to address such issues was the Space Power Experiments Aboard Rockets (SPEAR) series of experiments. SPEAR-I[10] was designed to measure whether or not the Earth's magnetic field impedes electron collection, SPEAR-II to test pulsed high-voltage components, and SPEAR-III[17] to test proposed spacecraft grounding mechanisms. An analysis of the bipolar sheath using NASCAP/LEO (and POLAR) was published[10]. We compare key published results with results computed using *Nascap-2k*.

The PATRAN object originally used for the NASCAP/LEO calculations and used here for a *Nascap-2k* calculation is shown in Figure 9. It consists of gold-plated spheres mounted on cylindrical nickel booms. The nickel booms are bushings constructed with grading rings that are connected by resistors. The graded boom created a uniform potential gradient from the positively biased sphere to payload ground. The booms are connected to a cylindrical support boom covered with plastic. This boom is in turn connected to the main (aluminum) rocket body.

Nascap-2k requires a finer resolution computational grid around the spheres than that used in the earlier NASCAP/LEO calculations. Five nested grids, with an outer grid resolution of 1.1 m and an inner grid resolution of 0.06875 m, were used in the *Nascap-2k* calculations.

The calculations use a density of 5×10^{10} m^{-3}, a temperature of 0.1 eV, and Oxygen ions. The 0.4 Gauss magnetic field is normal to the plane determined by the spheres and the axis of the body. *Nascap-2k* provides a selection of space charge density models. As this is a steady-state calculation in a short Debye length motionless plasma, the non-linear analytic space charge density model, including convergence, is used.

The *Nascap-2k* and NASCAP/LEO potential calculations give similar results. Figure 10 and Figure 11 show space potential contours as computed by the two codes for the same applied potentials. The shapes and locations of the contour levels are the same. Figure 12 and Figure 13 show sample electron trajectories as computed by the two codes. The differences in the trajectories are due to the differences in the potential solution (different grid structure and interpolation functions) and the initial position of the trajectory.

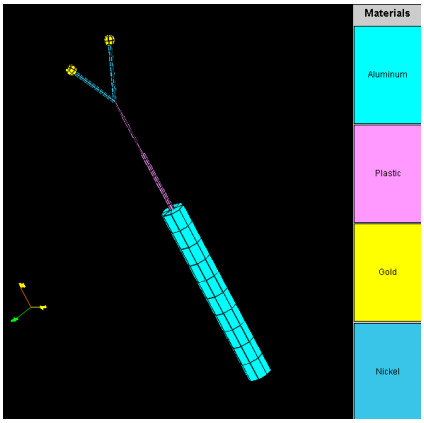

Figure 9. PATRAN model of SPEAR I used for the study of current collection in a bipolar sheath in a low-earth-orbit environment.

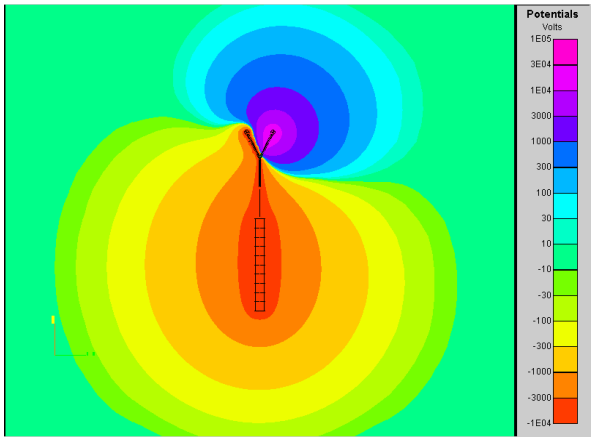

Figure 10. Nascap-2k potential contours with one sphere at +46 kV with respect to spacecraft ground and spacecraft ground at –6 kV.

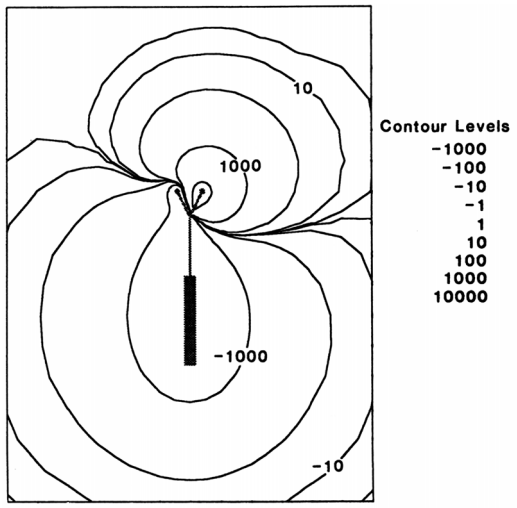

Figure 11. NASCAP/LEO potential contours for one sphere at +46 kV with respect to spacecraft ground and spacecraft ground at –6 kV.10 Reproduced by permission of American Geophysical Union.

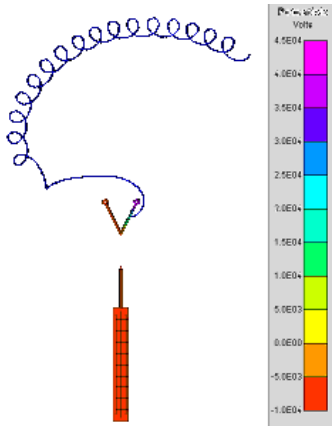

Figure 12. Sample electron trajectory in potential contours shown in Figure 10.

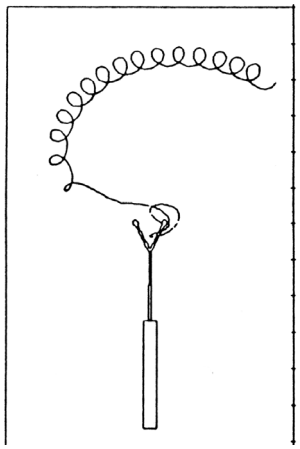

Figure 13. Sample electron trajectory in potential contours shown in Figure 11 .[10] Reproduced by permission of American Geophysical Union.

Table 5. Calculated Chassis Floating Potential and Current as computed by NASCAP/LEO and *Nascap-2k*.

Sphere Bias (kV)	Chassis floating potential (kV)		Sphere and bushing current (mA)	
	LEO	N2k	LEO	N2k
46	–8.3	–5.9	45.2	40.6
24	–5.3	–3.9	26.9	21.6
12	–3.3	–2.6	13.4	10.9
1	–0.6	–0.58	1.4	0.61

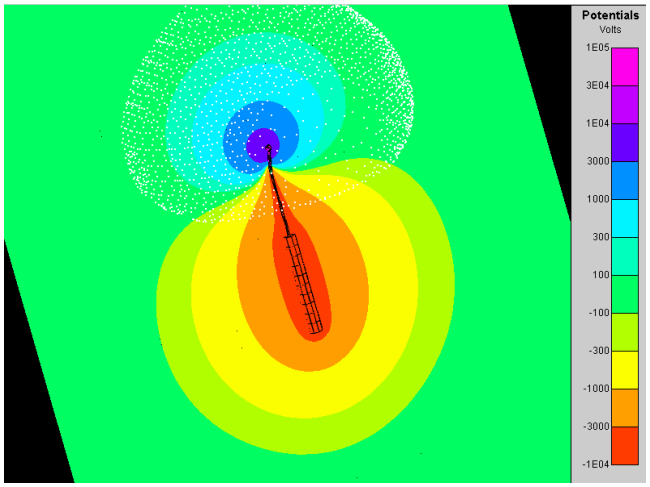

Figure 14. The white dots show the electron sheath edge with 46 kV bias and –8.3 kV chassis potential as computed by *Nascap-2k*.

Reference 10 compares NASCAP/LEO calculations with flight measurements of the spacecraft ground floating potential and the current collected by the biased sphere as a function of the bias value. The high energy cutoff in the ion flux spectra of the energetic particle detectors gives the floating potential. The width of the peak limited the accuracy of the floating potential measurement to within only an order of magnitude. The NASCAP/LEO results are near the center of the range.

The NASCAP/LEO and *Nascap-2k* calculated floating potentials and sphere and bushing currents are given in Table . The *Nascap-2k* floating potentials are slightly less as the electron currents computed by *Nascap-2k* are about one-third those computed by NASCAP/LEO for the same potentials. This is a result of the reduction in sheath current due to the magnetic field, a phenomenon that is not accounted for in NASCAP/LEO. Figure 14 shows the location of the

electron sheath. The magnetic field limits the plasma thermal current entering the sheath from the top, significantly reducing the electron current.

The measured collected electron current as a function of applied bias can be fit by a line I(mA) = 0.880 V(kV). The NASCAP/LEO results can be fit by a line I(mA) = 0.985 V(kV). The *Nascap-2k* results can be fit by a line I(mA) = 0.886 V(kV). The *Nascap-2k* currents as a function of floating potential agree with the flight measurements even better than the earlier NASCAP/LEO results do.

Auroral Spacecraft Charging

To validate *Nascap-2k* for auroral charging, a comparison of results obtained using *Nascap-2k* with those obtained using POLAR for the Defense Meteorological Satellite Program spacecraft (DMSP) was done.[25] The DMSP spacecraft definition used for the calculations described in Reference 25 was used for the *Nascap-2k* calculations.

Charging in eclipse from an initial potential of –10 V was computed for a period of 6 s with 45 timesteps varying from 0.0125 s to 0.2 s. In all cases, the charging currents were computed using an analytic model for the electrons and tracked ions. The charge density can be computed either analytically or self-consistently with the ion trajectories. In the first case, the ion currents are computed by tracking macroparticles from the sheath and in the second case by tracking macroparticles from the boundary of the computational space. The environment is described by a low energy plasma and high energy auroral electrons. The low energy plasma is a Maxwellian. The high energy electrons are described by a three component Fontheim[26] distribution.

$$\mathrm{Flux}_{\mathrm{Font}}(E) = \sqrt{\frac{e}{2\pi\theta_{\max} m_e}}\,\frac{E}{\theta_{\max}}\, n \exp\left(-\frac{E}{\theta_{\max}}\right) + \pi\zeta_{\mathrm{gauss}} E \exp\left(-\left(\frac{E_{\mathrm{gauss}} - E}{\Delta}\right)^2\right) + \pi\zeta_{\mathrm{power}} E^{-\alpha}$$

The plasma environment parameters used are shown in Table 6. The spacecraft is moving at 6565 m/s in the –X direction.

Calculations can be done for two different charge density models: the analytic charge density model used in the SPEAR I calculation, and the self-consistent with ion trajectories model. We used the second charge density model as it is more appropriate for moving spacecraft. Ions are tracked from the problem boundaries and their spacecharge deposited on grid nodes at each step. Each ion is tracked until it reaches the spacecraft or leaves the grid. After the tracking step, the charge density is computed from the resulting ion density and a barometric description of the electrons.

Table 6. Parameters used to describe auroral environment.

Low energy plasma	**Density**	3×10^{9} m^{-3}
	Temperature	0.2 eV
	Hydrogen fraction	9%
High energy electrons		
Maxwellian component	**Density**	2.49×10^{5} m^{-3}
	Temperature	3200 eV
Gaussian component	**Coefficient**	1.5×10^{4}
	Energy	3.5×10^{4} eV
	Width	1.8×10^{4} eV
Power law component	**Coefficient**	2×10^{10}
	Minimum energy	50 eV
	Maximum energy	1.6×10^{6}
	Exponent	1.05

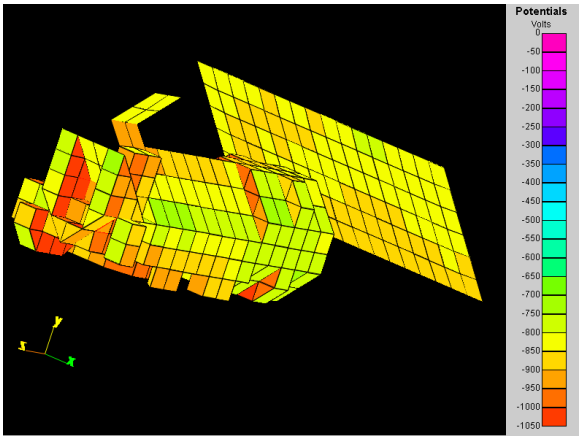

Figure 15. Resulting surface potentials for case with self-consistent charge density computed by *Nascap-2k*.

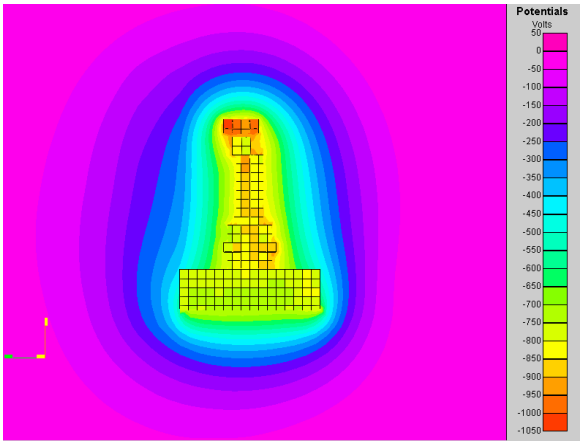

Figure 16. Resulting space potentials for case with self-consistent charge density computed by Nascap-2k.

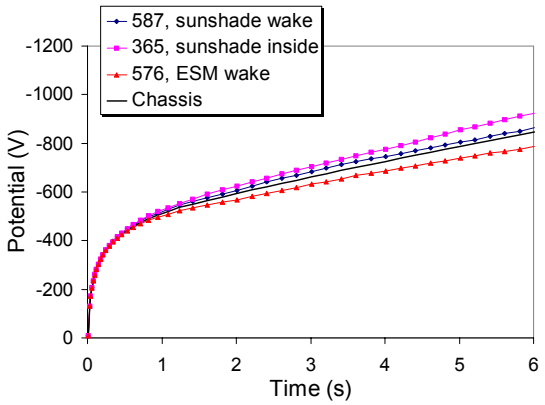

Figure 17. Time history of charging with self-consistent charge density computed by Nascap-2k.

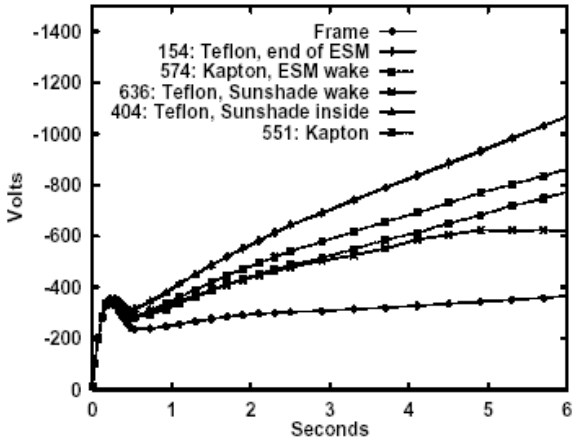

Figure 18. Figure 5 of Reference 25.

The results of the calculations are given in Figure 15 through Figure 17. With these choices for parameters, the resulting chassis potential is –845 V and surface potentials vary between –710 and –1025 V. The well-shadowed surfaces are the most negative. The chassis rapidly charges to the –500 V level and continues to charge at about 60 V per second. With more timesteps, the results might be slightly different.

These results can be compared with Figure 5 of Reference 25, shown here as Figure 18. The *Nascap-2k* results do not have the, presumably spurious, hump at 0.2 sec, show more charging, and are continuing to charge. The charging of the surfaces with respect to each other is not the same, but as the selected surfaces are probably different, no firm conclusions can be drawn.

Another set of calculations in the same paper was also repeated. The thickness of Teflon was set to 2.8×10^{-3} and all the Kapton was changed to Teflon. The results are shown in Figure 19 through Figure 21. These results can be compared with Figure 22 through Figure 24 obtained from POLAR. Again, the results using the two codes are similar in character. The shaded surfaces are the most negative and the ram-wake difference is small. Using POLAR, the wake side charges more than the ram side. Using *Nascap-2k*, the ram side charges slightly more than the wake side. The incident ions are focused onto the wake side of the spacecraft. The *Nascap-2k* and POLAR auroral charging results have the same character.

Conclusions

Nascap-2k is already proving valuable with its improved geometric modeling and surface electric field accuracy. It can be used to do the highest accuracy three-dimensional spacecraft-plasma interaction calculations with a single, straight-forward user interface. Calculations of interactions of a sphere with a surrounding plasma using *Nascap-2k* are consistent with analytic solutions. *Nascap-2k* reproduces or improves upon results from NASCAP/GEO, NASCAP/LEO, and POLAR for a selection of typical interactions calculations. *Nascap-2k* includes the limitation of collected current due the magnetic field in low-earth-orbit problems and provides much improved geometric and time fidelity in tenuous charging calculations.

Nascap-2k can be obtained from NASA's SEE Program. Contact Jody Minor, jody.minor@nasa.gov or David Cooke david.cooke@hanscom.af.mil (Air Force users).

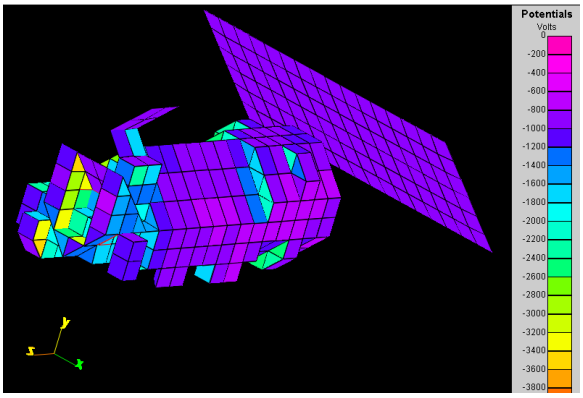

Figure 19. Resulting surface potentials for case with all Teflon and self-consistent charge density computed by *Nascap-2k*.

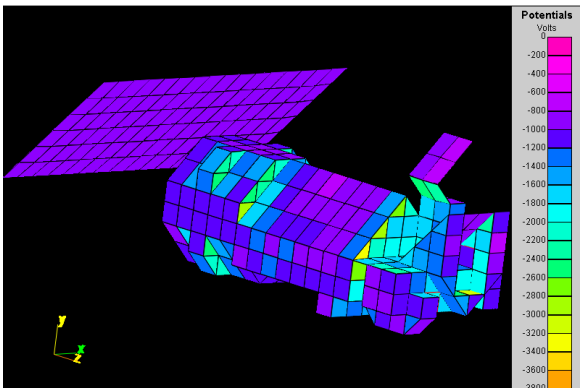

Figure 20. Resulting surface potentials for case with all Teflon and self-consistent charge density computed by *Nascap-2k*.

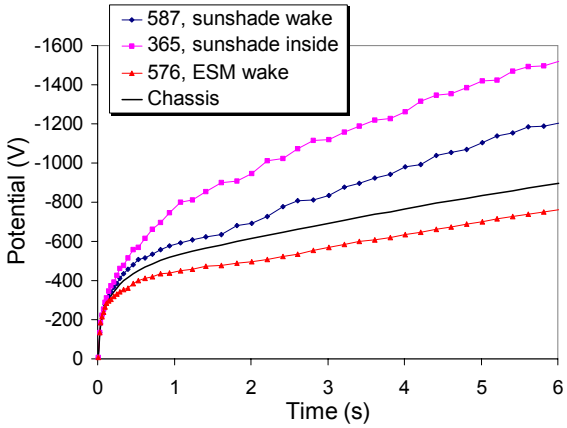

Figure 21. Time history of charging with all Teflon and self-consistent charge density computed by *Nascap-2k*.

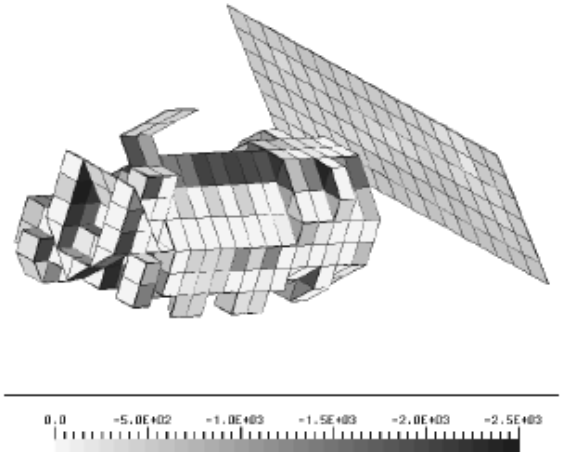

Figure 22. Resulting surface potentials using POLAR for Teflon only case from Reference 25.

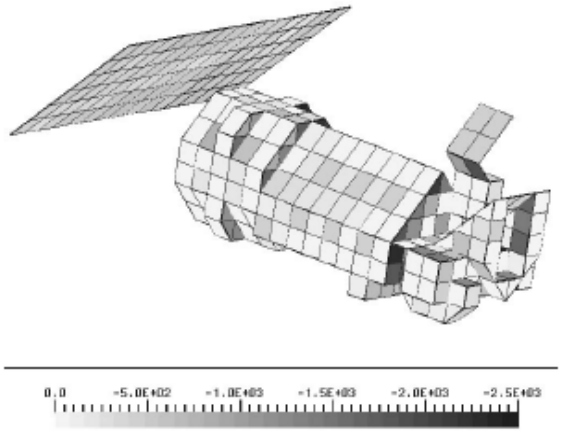

Figure 23. Resulting surface potentials using POLAR for Teflon only case from Reference 25.

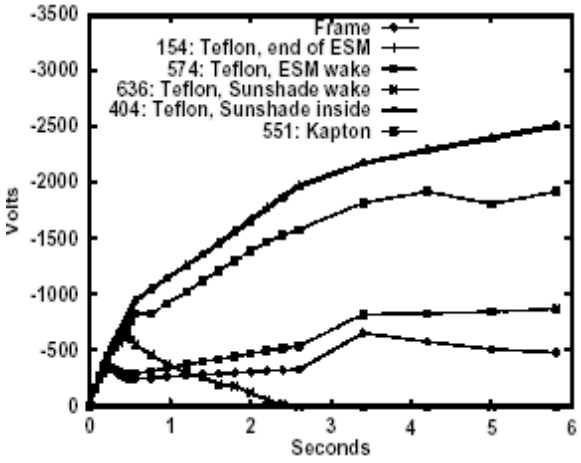

Figure 24. Time history of surface potentials using POLAR for Teflon only case from Reference 25.

Ackowlegements

Nascap-2k is jointly funded by the Air Force Research Laboratory and NASA's Space Environments and Effects (SEE) Program. This paper was written under contract with the Air Force Research Laboratory.

References

1. M.J. Mandell, I. Katz, J.M. Hilton, J. Minor, D.L. Cooke, *Nascap-2k*, A Spacecraft Charging Analyis Code for the 21st Century, AIAA Paper 2001-0957, *AIAA Aerospace Sciences Meeting & Exhibit, 39th, Reno, NV,* Jan. 2001.

2. M.J. Mandell, I. Katz, D. Cooke, *Towards a more robust spacecraft charging algorithm*, AIAA Paper AIAA 99-0379, 1999.

3. M.J. Mandell, V.A. Davis, B.M. Gardner, I.G. Mikellides, D.L. Cooke, J. Minor, *Nascap-2k*—An Overview, This proceedings.

4. V. A. Davis, L. F. Neergaard, M.J. Mandell, I. Katz, B.M. Gardner, J. M. Hilton, J. Minor, *Spacecraft Charging Calculations: Nascap-2k and SEE Interactive Spacecraft Charging Handbook*, AIAA Paper, AIAA 2002-0626, 2000.

5. M.J. Mandell, P.R. Stannard, I. Katz, *NASCAP Programmer's Reference Manual,* NASA CR 191044, 1993.

6. P.R. Stannard, I. Katz, L. Gedeon, J.C. Roche, A.G. Rubin, M.F. Tautz, *Validation of the NASCAP model using spaceflight data,* AIAA Paper AIAA 82-0269, 1982.

7. I. Katz, P.R. Stannard, L. Gedeon, J.C. Roche, A.G. Rubin, M. F. Tautz, NASCAP simulations of spacecraft charging of the SCATHA satellite, *Spacecraft/Plasma Interactions and their Influence on Field and Particle Measurements*, ESA SP-198, p. 109, 1983.

8. I.Katz, D.E. Parks, M.J. Mandell, J.M.Harvey, S.S. Wang, J.C. Roche, NASCAP, a three-dimensional charging analyzer program for complex spacecraft, *IEEE Trans. Nucl. Sci., NS-24*, p. 2276, 1977.

9. M.J. Mandell, and I. Katz, *High Voltage Plasma Interactions Calculations Using NASCAP/LEO*, AIAA Paper AIAA-90-0725, 1990.

10. I.Katz, G.A. Jongeward, V.A. Davis, M.J. Mandell, R.A. Kuharski, J.R. Lilley, Jr., W.J. Raitt, D.L. Cooke, R.B. Torbert, G. Larson, and D. Rau, Structure of the Bipolar Plasma Sheath Generated by SPEAR I, *J. Geophys. Res., 94*, A2, p. 1450, 1989.

11. M.J. Mandell, V.A. Davis, *User's Guide to NASCAP/LEO*, S-CUBED Division of Maxwell Laboratories, SSS-R-85-7300-R2, 1990.

12. T. Neubert, M.J. Mandell, S. Sasaki, B.E. Gilchrist, P.M. Banks, P.R. Williamson, W.J. Raitt, N.B. Meyers, K.I. Oyama, I. Katz, The sheath structure around a negatively charged rocket payload, *J. Geophys. Res., 95*, p. 6155, 1990.

13. M.J. Mandell, J.R. Lilley, Jr., I. Katz, T. Neubert, N.B. Myers, Computer modeling of current collection by the CHARGE-2 mother payload, *Geophys. Res. Lett., 17*, p. 135, 1990.
14. J.R. Lilley, Jr., D.L. Cooke, G.A. Jongeward, I. Katz, *POLAR User's Manual*, GL-TR-89-0307, 1989.

15. M.J. Mandell, T. Luu, J. Lilley, G. Jongeward, and I. Katz, *Analysis of Dynamical Plasma Interactions with High Voltage Spacecraft,* (2 volumes), Rep. PL-TR-92-2258, Phillips Lab., Hanscom Air Force Base, MA, 1992.

16. V.A. Davis, M.J. Mandell, D.L. Cooke, C.L. Enloe, High-voltage interactions in plasma wakes: Simulation and flight measurements from the Charge Hazards and Wake Studies (CHAWS) experiment, *J. Geophys. Res., 104,* A6, p. 12445, 1999.

17. M.J. Mandell, G.A. Jongeward, D.L. Cooke, W.J. Raitt, SPEAR 3 flight analysis: Grounding by neutral gas release and magnetic field effects on current distribution, *J. Geophys. Res., 101*, A1, p. 439, 1998.

18. M.J. Mandell, I. Katz, P.G. Steen, G.W. Schnuelle, The effect of solar array voltage patterns on plasma power losses, *IEEE Trans. Nucl. Sci., NS-27*, p. 1797, 1980.

19. D.L. Cooke, I. Katz, M.J.Mandell, J.R. Lilley Jr., and A.J. Rubin, Three-Dimensional Calculation of Shuttle Charging in Polar Orbit, *Proc. of the Spacecraft Environmental Interactions Technology Conference 1983*, ed by Carolyn K. Purvis and Charles P. Pike, NASA Conf. Pub. 2359, AFGL-TR-85-0018, p. 205, 1985.

20. I. Langmuir, K.B. Blodgett, Currents limited by space charge between concentric spheres, *Phys. Rev., 24*, p. 49, 1924.

21. L.W. Parker, B.L. Murphy, Potential buildup on an electron-emitting ionospheric satellite, *J. Geophys. Res., 72,* p. 1631, 1967.

22. This section originally published in Reference 4 copyright © by the American Institute of Aeronautics and Astronautics, Inc. Reprinted with permission.

23. I. Katz, V.A. Davis, M.J. Mandell, B.M. Gardner, J.M. Hilton, J. Minor, A.R. Fredrickson, D.L. Cooke, *Interactive spacecraft charging handbook with integrated updated spacecraft charging models*, AIAA paper AIA 2000-0247, 2000.

24. C.K. Purvis, H.B. Garrett, A.C. Whittlesey, N.J. Stevens, *Design guidelines for assessing and controlling spacecraft charging effects*, NASA TP 2361, p. 3, 1984.

25. D.L. Cooke, Simulation of an Auroral Charging Anomaly on the DMSP satellite, 6^{th} *Spacecraft Charging Technology Conference,* AFRL-VS-TR-20001578, 2000.

26. E.G. Fontheim, K. Stasiewicz, M.O. Chandler, R.S.B. Ong, E. Gombosi, R.A. Hoffman, Statistical study of precipitating electrons, *J. Geophys. Res., 87*, p 3469, 1982.